Proceedings of the IASS 2024 Symposium
Redefining the Art of Structural Design
August 26-30, 2024, Zurich Switzerland
Philippe Block, Giulia Boller, Catherine DeWolf,
Jacqueline Pauli, Walter Kaufmann (eds.)

Towards the control of doubly curved active textiles through graded pre-stretching and 3D printing

Sebastian LETTNER*[a], Marco PALMA[a], Efilena BASETA[a]

*[a]
Institute of Art and Design E264/2, Faculty of Architecture and Planning,
Technische Universität Wien, Karlsplatz 13, 4th Floor, 1040 Vienna, Austria
sebastian.lettner@tuwien.ac.at

Abstract

The production of complex shell geometries with the aid of textile supports is of interest in various fields, from fashion design to architecture, and at various scales of application. Yet, digital fabrication methods addressing double-curved shells by means of pre-stretched textiles and 3D-printing currently lack solutions for systematically controlling the curvature of the fabricated components. We introduce two methods for activating and controlling the double curvature of square tile elements by means of a custom-designed digital fabrication set-up. The set-up consists of a standard 3D printer integrated with a bespoke numerically controlled actuator for textile pre-stretching. The first method couples a non-uniform pre-stretching of the textile and a uniform cross section of the 3D printed boundary. The second method involves the combination of a uniform pre-stretching and non-uniform cross-section across the tile boundary. We independently evaluate the two methods and compare them in terms of effectiveness and repeatability in the activation of the tile curvature, specifically focusing on the edge conditions of the fabricated tile components. Finally, we discuss the possibility for large-scale applications and the potential for further research.

Keywords: active textiles, double-curved shells, non-uniform stretching, 3D printing, non-uniform printing thickness

1. Introduction

1.1. State of the art

In the architecture and construction sector, the production of complex curvature elements and components often relies on the fabrication of complex molds and formworks, rendering such a process costly, time- and energy-consuming [1]. In the last decades, architects, engineers and researchers have been exploring more and more efficient methods for the design and fabrication of such geometries. These methods are addressed to the production of both molds, formworks and jigs, or to the fabrication of self-standing shells and spatial structures [2] [3]. By leveraging the material inherent properties, it is possible to generate complex geometries even more efficiently. For example, the simultaneous use of bending and contracting elements can lead to the production of doubly curved structures without (or with a limited need for) molds and formworks [4] [5]. An alternative way to address the production of bending-active system involves the direct fabrication of a composite material structure through 3D printing on a pre-stretched elastic fabric. This method is usually referred to as “4D printing”, “Active Textiles” or “Programmable Textiles”. Several active textile production methods rely on standard FDM 3D printers, and have been successfully employed in prior design-related research, but without addressing the topic of fabrication repeatability [6]. Prior research also focused on the complex task of developing accurate digital tools for the simulation and prediction of such complex composite material behaviors [7][10]. At

the moment, similar models can only manage the simulation of uniform fabric pre-stretching conditions, either uniaxially, biaxially or radially [6]. Active textile methods have so far efficiently addressed small-scale applications, such as the rapid prototyping of shell structures [7]. When tackling the architectural scale, researchers' attention shifted towards other means of production. The use of fiber placement technologies to form large-spanning shell structures with sewn-in carbon fiber rods [8] or lamination processes with different materials like latex and plywood to enable surface activation [9] were investigated. At the moment, the process of upscaling active textile methods requires further investigations into the underlying material parameters, as well as uniform testing standards, and production technology [6]. Reproducing a simulated, anticipated geometry has not yet been explored to a degree where curvature can be reliably controlled [10]. More recently, the use of hinges and of buckling - created through sudden changes in the cross section of the 3D printed element –were introduced as methods to induce shape variation in active textiles [11].

1.2. Aim of research

The aim of this research is to introduce, evaluate and compare two novel fabrication methods for a controlled activation of the double curvature of pre-stretched textile square tile components. Through the controlled bending of the 3D printed boundary by the pre-stretched textile the defined processes can control the curvature without adding material on the surface of the piece except the edges. Enhancing the control over the resulting curvature at the edges of the tiles leads to a reliable way to fine-tune sample production and ensures a high degree of repeatability. Both methods (see 2.2) are enabled by the development of a custom-built digital fabrication setup, which integrates numerically controlled textile stretching and FDM 3D printing (see 2.1). By introducing a higher degree of control in the textile curvature activation, not only do we contribute to the advancement of prior active textile fabrication processes, but we also provide comparable data for further research developments.

2. Methodology

To introduce control in the production of doubly curved active textile components, we developed a custom-made digital fabrication set-up. The set-up allowed us to run a series of systematic material experiments to evaluate the relationship amongst fabrication process parameters - i.e. textile pre-stretching, 3D printed boundary geometry and resulting tile element curvature. We established systematic digital and physical post-production processes, as well as a 3D scanning routine to obtain comparable and reproducible data. We used computational design methods to efficiently design the digital input geometries, as well as to extract curvature information from the captured physical samples. In the following paragraphs, we offer a detailed overview of our custom-made fabrication (2.1) and measuring (2.3) set-ups, and we introduce the methods used to induce and evaluate curvature in active textiles tile components (2.2).

2.1. Fabrication Set-Up

As shown in Figure (1), the set-up is built upon a standard desktop FDM 3D printer (brand Creality, model Ender 3) integrated with a custom-designed numerically controlled ground plate for textile pre-stretching.

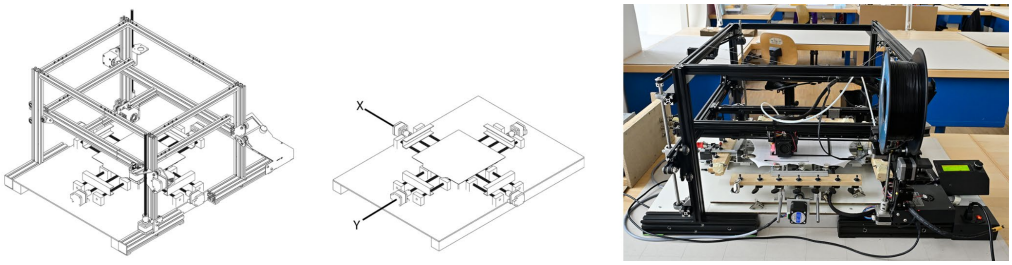

Figure (1): Fabrication Set-Up, left: 3D-model of machine, mid: 3D-model of custom-made ground plate, right: image of set-up

The ground plate is a flat steel plate mechanically fixed to the 3D printer heated bed and measures 235x235x2 mm. It includes two orthogonal clamping and pulling mechanisms oriented along the 3D

printer X and Y axes. The clamping of the textile happens mechanically, while the pulling mechanism is computer controlled. The clamping mechanism is designed to allow for both linear and pointwise clamping on the 4 edges of the textile. In the linear clamping configuration, the whole edge of the textile is clamped lengthwise. In the pointwise clamping option, each edge of the textile is clamped at 7 evenly spaced locations by independent pins. The pulling mechanism relies on 2 opposing sets of threaded spindles (8 mm diameter, 2 mm pitch) with two additional linear guide rails, and on 2 opposing pairs of Nema17 stepper motors, also aligned to the X and Y axes. The setup is controlled by an Arduino UNO with a CNC shield and four TB6600 stepper controllers. The maximum pulling distances are 150 mm for pointwise clamping and 160 mm for linear clamping for each edge.

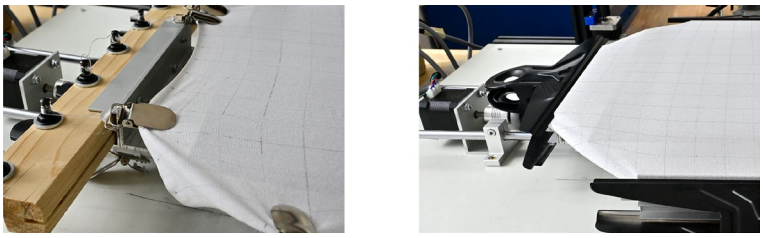

Figure (2): Clamping methods, left: pointwise, right: linear

2.2. Material experiments

Given the size and the physical constraints of our fabrication set-up, we conducted a set of material experiments on square tiles with dimensions 180x180 mm. The experiments focused on testing repeatability (see 2.2.2) and effectiveness in terms of curvature-activation of two different production strategies (see 2.2.3 and 2.2.4) afforded by our fabrication setup. The first strategy couples a non-uniform pre-stretching of the textile and a uniform cross section of the 3D printed boundary. The second method involves the combination of a uniform pre-stretching and non-uniform cross-section across the tile boundary. In all the experiments, we used viscose jersey fabric and PLA filament for 3D printing. Material specifications are displayed in table (1). To ensure good printing quality and sufficient adhesion of the PLA to the textile, we employed 3D printing settings suggested in previous research and detailed in table (2) [12]. To isolate the impact of the pre-stretching and of the boundary cross section on the activated sample tiles, we kept the 3D printing settings and the boundary geometry identical throughout all the test runs. Similarly, the weave pattern of the textile is carefully and consistently oriented along the X and Y axis of the set-up.

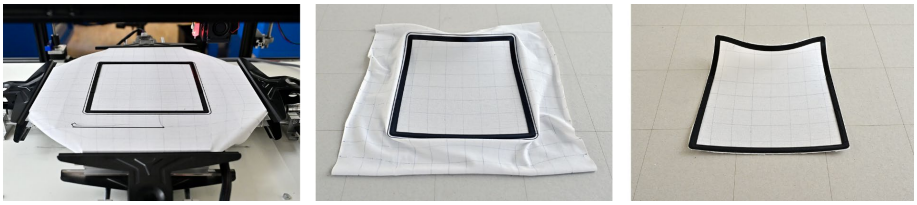

Figure (3): Example of post-printing process, from finished print to final tile

As illustrated in Figure (3), each 3D printing experiment followed a specific post-production procedure. After completing each print, the output is left in its clamped and stretched configuration for 10 minutes. The fabric is un-clamped, and the tile placed on a table for 30 minutes with the excess fabric still around the 3D printed frame. Finally, the excess fabric is carefully cut by hand with a Stanley knife.

Table (1): Material properties and geometry of fabric and PLA

	Material	Weight	Thickness	Geometry
Fabric	92% viscose, 8% elastane	220g/m²	0.3mm	280mm x 280mm
PLA	Geeetech Pure PLA		1.75mm	180mm x 180mm, 7.5mm wide, 0.7mm high

Table (2): Print settings of 3D printer for every experiment

			Layer Hight			
Hot End	Flow	Speed	Initial	Rest	Infill	z-Probe Offset
210°C	105%	25mm/s	0.15mm	0.2mm	100%	1.625mm

2.2.1. Uniform pre-stretching and uniform boundary cross section

To test the repeatability of our fabrication methods, we produced 3 sample tiles with identical design and fabrication parameters, i.e. type of clamping, textile pre-stretching, 3D printing parameters and boundary geometry. The applied amount of pre-stretch was 75 mm in both X and Y directions (corresponding to a 25% stretch of the initial textile size and a force of 22,50 N). The textile was linearly clamped to the ground plate. The boundary has a uniform cross section (see Table 1 for details), and with parameters shown in Table 2.

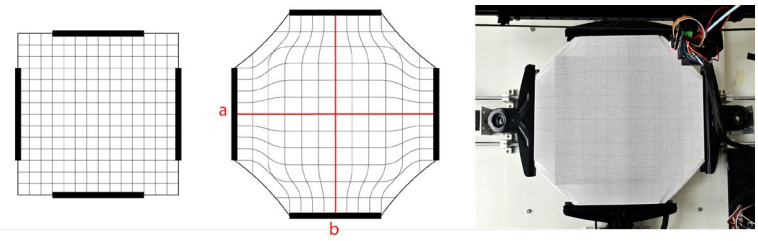

Figure (4): visualization of uniform pre-stretching and linear clamping

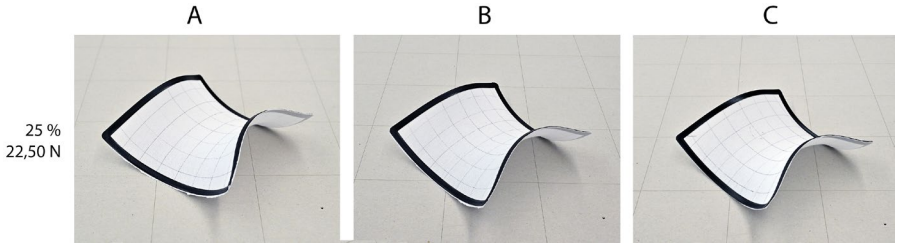

Figure (5): produced tiles - uniform pre-stretching (25% / 22,50 N) and uniform boundary cross sections

2.2.2. Non-uniform textile pre-stretching

The first of the two fabrication methods we introduce assumes that by applying a non-uniform pre-stretching along the textile boundary we can inform changes in the curvature of the resulting sample tiles. We conducted a series of experiments to demonstrate the possibility to control the overall surface curvature by only acting on one specific edge of the tile. We thus pre-stretched the fabric according to a trapeze-shaped diagram using the point-wise clamping mechanism (see Figure 6). Consistently to 2.2.1, the geometry of the 3D printed boundary is described in Table 1 and has uniform cross section. We ran two different test runs focusing on the activation of the same edge: one for testing repeatability, one for testing variability. Repeatability was tested by producing three samples with a maximum pre-stretch of 90 mm (30% of the initial textile edge length) along axis ‘a’ (see figure 7 – top) pulled with a force of 3,72 N. Variability in resulting curvature was tested by producing three more samples as shown in figure 7 - bottom with 20% / 1,45 N, 40% / 10,90 N and 50% / 30,21 N pre-stretching on one edge. See Table 3 for detailed information.

Table (3): variable fabrication parameters of non-uniform pre-stretching tiles

Fabric	20% stretch: a= 60mm, b= 10mm, c=12mm; F(a) = 1,45 N
	30% stretch: a = 90mm, b= 10mm, c=12mm; F(a) = 3,72 N
	40% stretch: a = 120mm, b= 10mm, c=12mm; F(a) = 10,90 N
	50% stretch: a = 150mm, b= 10mm, c=12mm; F(a) = 30,21 N

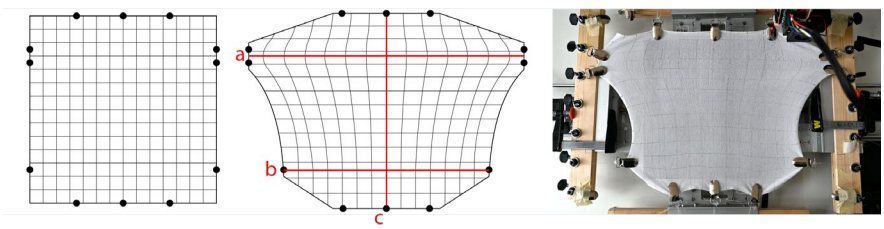

Figure (6): visualization of non-uniform pre-stretching and pointwise clamping

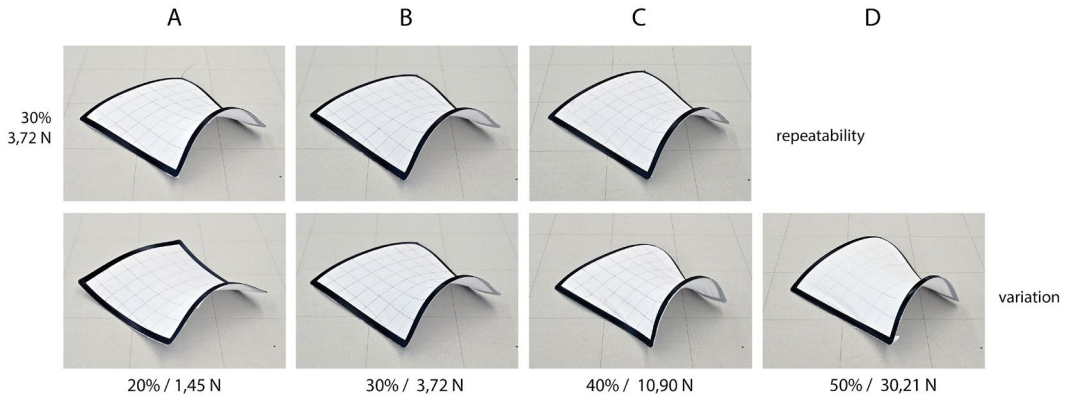

Figure (7): produced tiles – non-uniform pre-stretching top: repeatability test, bottom: test with variable pre-stretching parameter and resulting curvature

2.2.3. Non-uniform boundary cross section

The second fabrication method we introduce, complementary to the one described in 2.2.2, assumes that by keeping the textile pre-stretching constant along the four edges, and by locally adjusting the geometry of the 3D printed boundary, we can inform the bending resistance of the tile edges and thus the overall surface curvature. As in 2.2.2, we produce three samples to test the repeatability (see figure 9 – top) and three more to test variability (figure 9 – bottom). All tests relied on a uniform pre-stretching of 75 mm (25% of the initial length) in both axis (same as 2.2.1 and 2.2.2) pulled with a force of 22,50 N. A simple parametric model defines the cross section variability of the printed boundary, which is divided into sections of variable number and height, as shown in Figure 8. This simple model allows control of the curvature in a particular area of the tile and at a particular edge. The geometric features of the three different boundaries are described in Table 4.

Table (4): variable fabrication parameters of non-uniform boundary cross section

Border	Height: a = 0.5mm, b = 0.9mm, c = 1.3mm
	Height: a = 0.8mm, b = 1.2mm, c = 1.6mm
	Height: a = 1.1mm, b = 1.5mm, c = 1.9mm

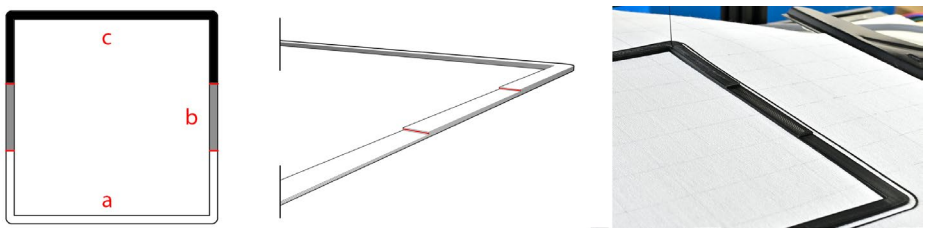

Figure (8): visualization of non-uniform boundary cross section

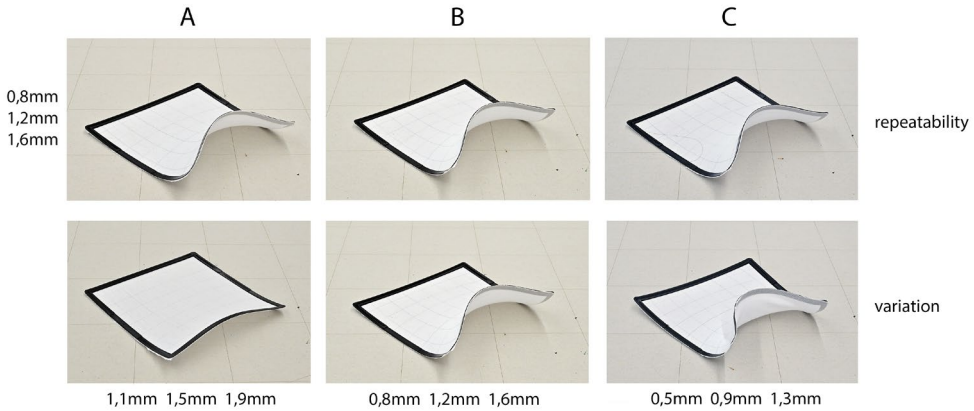

Figure (9): produced tiles – non-uniform boundary cross section, top: repeatability test, bottom: test with variable boundary cross section parameter and resulting curvature

2.3. Evaluation process

To evaluate the geometry produced by the abovementioned methods, we measured the physical sample tiles via 3D scanning. Specifically, we used an Intel RealSense L515 LiDAR camera with 1024x768 pixels depth sensor resolution, statically positioned relative to the samples (figure 10 – left and middle). We automated the capturing and post-processing of the depth data with the RS_GH plugin [13] for McNeel Rhinoceros/Grasshopper environment, used to convert raw point cloud data to untrimmed N.U.R.B.S. surfaces. For each sample surface/tile we measured 1) the z-displacement and rendered it as a greyscale image, and 2) the Gaussian curvature of the overall tile and render it as a color gradient map. Additionally, we extracted and compared the corresponding surface edges according to repeatability and variability based on maximum deviation and local curvature values.

Figure (10): left and middle: scanning procedure with Intel RealSense L515 LiDAR camera; right: uniform stretching with dual-axis membrane testing machine with linear clamping

Furthermore, we custom-built a dual-axis membrane testing machine (figure 10 – right) to measure 1) the pre-stretching force applied to the textile before printing and 2) the residual stretching force stored in the already activated tile. We automated the post-processing and visualization of the data stored in the machine in the McNeel Rhinoceros/Grasshopper environment. The machine uses: s-type load cells with a force range of 50 N mounted on a framework designed in the same way as the ground plate of our fabrication set-up; 24bit delta-sigma DACs to digitize the signals coming from the load cells; a micro-controller to record the data and to control the stepper motors. We used a position-controlled testing procedure to evaluate the textile pre-stretching: the fabric was stretched to specific distances and in the procedure specific way matching the pre-stretching distances and type (uniform – nonuniform / linear – pointwise) used during tile production, as described in 2.2.1, 2.2.2, 2.2.3. To evaluate the residual amount of textile stretch in the activated tile we used the same machine setup, but with pointwise clamping. Each measurement results from the average of 5 repeated cycles of stretch and release of the fabric.

3. Results

We present and analyze the data collected from the previously described experiments, listed as corresponding sub-chapters.

3.1. Uniform pre-stretching and uniform boundary cross section

We notice a clear visual correspondence in terms of both z-displacement (figure 11 – top) and Gaussian curvature (figure 11 – bottom) across the three sample tiles. Generally, the results show a uniform activation of the whole tile surface, with a residual stretch force of 6,95 N stored in the activated tile. The Gaussian curvature analysis shows the largest deviations in the center of the test piece. The largest visible discrepancy is noticeable on surface C, where the highest positive curvature area on the top edge is shifted 12.2 mm towards the right side of the tile.

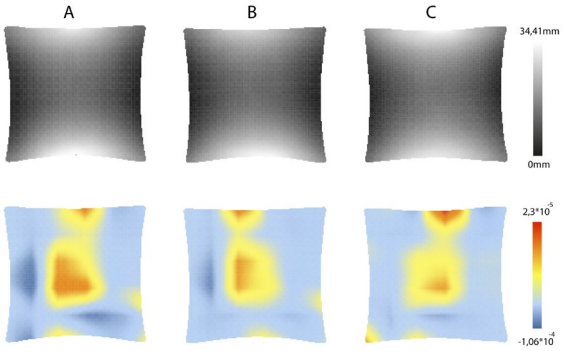

Figure (11): repeatability test - uniform stretching and uniform printing thickness – top: z-displacement evaluation of point cloud, bottom: Gaussian curvature analysis of N.U.R.B.S. surface

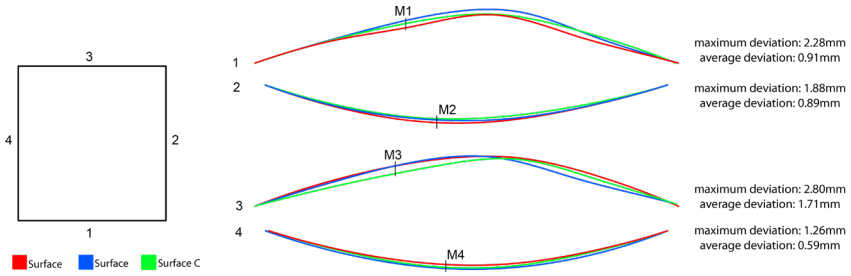

Figure (12): Analysis of edges – repeatability

Consistently to the curvature analysis, also the edge comparison highlights the above-mentioned shift on edge 3 on surface C. The peak of the curve on edge 1 is 8.5 mm out of center on every surface. The maximum deviation on edge 1 (point M1) and 3 (point M3) lies on 1/3 of the curve and on edge 2 (point M2) and 4 (point M4) it lies almost in the center. These offsets seem to associate opposing edges.

3.2. Non-uniform stretch

Corresponding to the repeatability test tiles shown in figure 7 - top and described in 2.2.2., the greyscale images (figure 13 – top) depicting the z-displacement show again overall similarities between the three surfaces. The Gaussian curvature analysis (figure 13 – bottom) as well as the z-displacement show the largest deviations in the center of the top edge. The largest visible discrepancy is noticeable on surface C, with the highest positive curvature area on the top edge. This corresponds to a slight deviation in the outlines as well. The comparison of the relevant edges of the tiles shows a maximum deviation of 2.27 mm and an average deviation of 0.97 mm for the repeatability test.

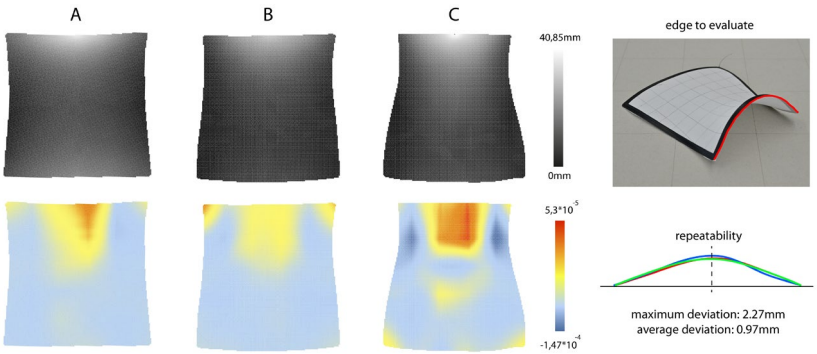

Figure (13): repeatability test – non-uniform pre-stretching– top: z-displacement evaluation of point cloud, bottom: Gaussian curvature analysis of N.U.R.B.S. surface

The greyscale images and the Gaussian curvature analysis in figure 14 are corresponding to the tiles shown in figure 7 – bottom and described in 2.2.2. Surface A to D are visually distinct from one another, especially between the mid and maximum amount of pre-stretching used. Gaussian curvature analysis confirms this, although showing some deviation for the 20% / 1,45 N pre-stretched panel (surface A). This surface forms a shape (see figure 7) comparable to the ones with uniform pre-stretching (see figure

5). We assume there is a certain threshold a tile with non-uniformly pre-stretched fabric needs to overcome to increase the curvature. This is shown as well by the graph in figure 15 mapping the resulting curvature and amount of pre-stretch. The Gaussian curvature analysis of Surface D shows a lot of imperfections and has its own boundary for evaluation. This is due to the textile starting to wrinkle with the use of 50% / 30,21 N pre-stretching and the sharp increase in resulting curvature. This shows the material limit of the used textile.

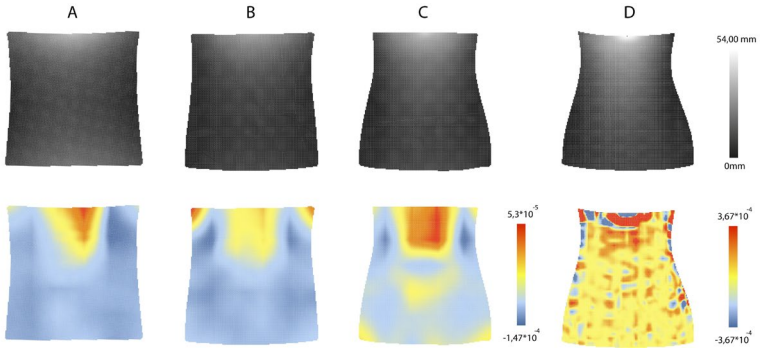

Figure (14): variable parameter of pre-stretching – non-uniform pre-stretching– top: z-displacement evaluation of point cloud, bottom: Gaussian curvature analysis of N.U.R.B.S. surface

The corresponding amount of curvature to the amount of pre-stretch is mapped in a graph showing exponential growth as well as the before mentioned threshold. Overall, the curves of the relevant edges show some imperfections regarding the symmetry.

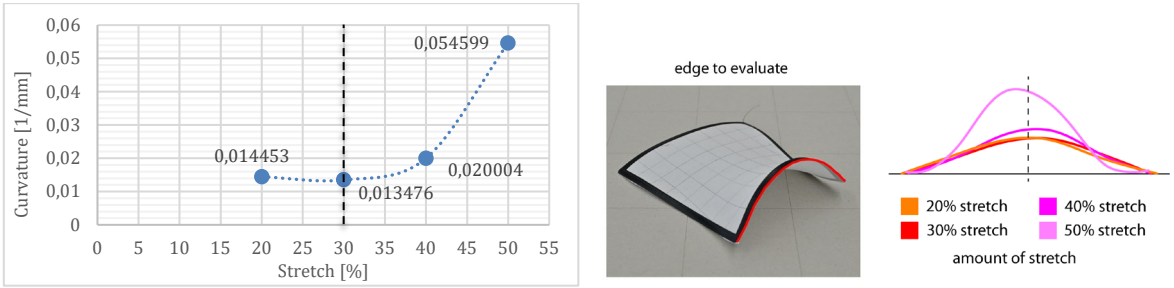

Figure (15): non-uniform pre-stretching - left: graph mapping curvature to amount of pre-stretch, right: analysis of edges

When evaluating the residual stretching force stored in the activated tiles, we notice a correspondence not only between curvature of the evaluated edge to the increase in pre-stretching (figure 15). The measured residual stretching force as well increases from 7,56 N at the tile with 30% = 90 mm pre-stretching to 11,96 N at the tile with 50% = 150 mm pre-stretching (figure 16).

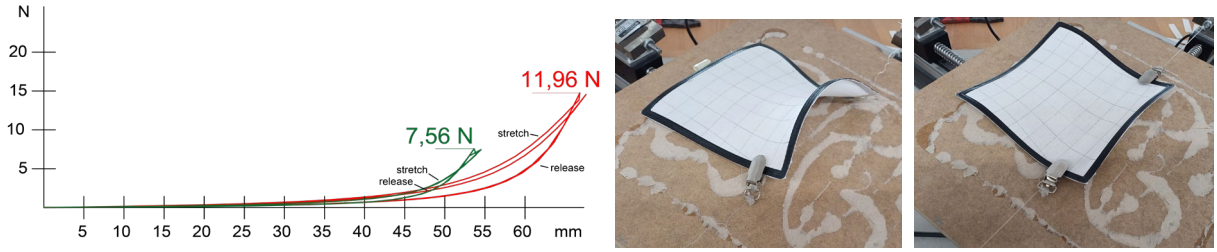

Figure (16): left: diagram of residual force of two tiles (red: 50% stretch, green: 30% stretch); right: images of method for testing residual force stored in activated tiles

3.3. Non-uniform boundary cross section

A steep incline at one edge with an otherwise flat tile as shown in figure 9 and described in 2.2.3. leads to a distinct gradient in the greyscale image. The bottom edge of the tiles highlighted in white in figure 17 – top shows this incline as z-displacement with some deviations between the surfaces. Due to 2/3 of the tile being flat the Gaussian curvature analysis shown in figure 17 - bottom gives limited amount of

data on the repeatability. The layered curves extracted from the relevant edge provide us again with data on the maximum and average deviation which correspond to the values measured before.

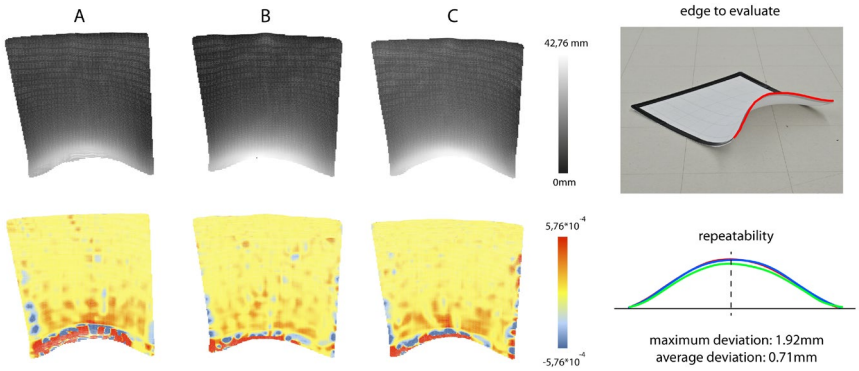

Figure (17): repeatability test – non-uniform boundary cross section – top: z-displacement evaluation of point cloud, bottom: Gaussian curvature analysis of N.U.R.B.S. surface

Investigating the correspondence between the printed boundary cross section and the resulting curvature shows a distinct outline of the tiles (figure 18) corresponding to the samples shown in figure 9 - bottom. We find the maximum z-displacement at surface B with the intermediate settings described in table 4. Due to the steep incline at surface C with the smallest boundary cross section is forming an overhang which explains the lower z-displacement at a higher curvature.

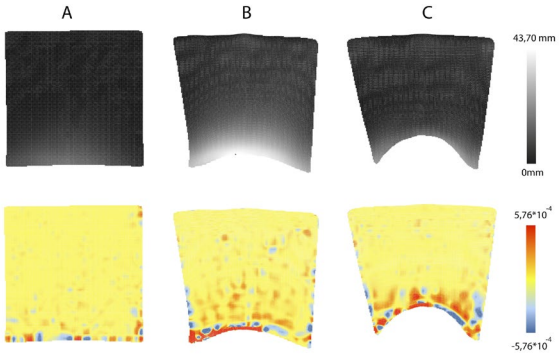

Figure (18): variable parameter of boundary cross section – non-uniform boundary cross section– top: z-displacement evaluation of point cloud, bottom: Gaussian curvature analysis of N.U.R.B.S. surface

We see almost linear behavior of the graph (figure 19) mapping the resulting curvature to the boundary height. In these experiments the curves show less imperfections and a great deal of symmetry.

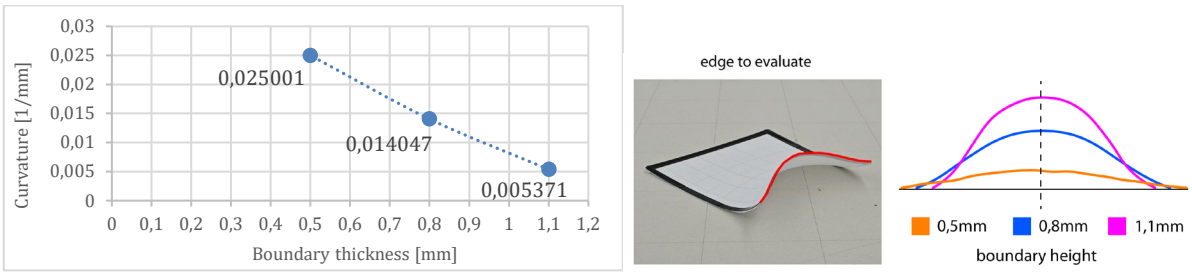

Figure (19): non-uniform boundary cross section - left: graph mapping curvature to cross section thickness, right: analysis of edges

When testing the activated tiles produced with the method of 'non-uniform boundary cross section' for residual force no comparable data could be gained due to the tiles having overhangs and folding in.

4. Conclusion

The proposed methods show promising results in controlling the curvature at the edges of the produced tiles. When using the presented fabrication set-up, uniform stretching with linear actuators and clamps

proof to be a reliable production routine regarding repeatability. The approach of non-uniform stretching the fabric shows potential in enhancing control over the resulting curvatures on the edges of active textile tiles, but the pointwise clamping mechanism is so far the weakest point of the set up regarding repeatability and control. This is where non-uniform thickness of the printed boundary steps in, leveraging the repeatability of uniform stretching. For now, the gained data regarding the geometry shows the most potential for the non-uniform boundary cross section and holds true for the specific fabric we used for producing the tiles, but with limited information on residual forces. Although the small scale of the size decided for the tiles, the gained insights can as well benefit larger scale and commercial application. Further research must be done exploring different materials, possible geometries, as well as evaluating curvature and stored residual force in activated tiles over time to elaborate on the desired curvature control. This can provide the possibility for scaling up this process and establish a fine-tuned procedure to create tiling structures.

References

[1] PERI. [Online]. Available: https://www.peri.ltd.uk/products/freeform-formwork.html

[2] L. Scheder-Bieschin, S. Bodea, M. Popescu, T. Mele, P. Block “A bending-active gridshell as falsework and integrated reinforcement for a ribbed concrete shell with textile shuttering: Design, engineering, and construction of KnitNervi” Structures, vol. 57, 2023

[3] J. Brütting, A. Körner, D. Sonntag, and J. Knippers, "Bending-active segmented shells," in Proceedings of the IASS Annual Symposium, Sep. 2017.

[4] S. M. Sabery, V. Soana, C. Bhaskar, and Y. Bayraktaoglu, "Elastic Choreographies: A robotic bending active structure interacting with humans," in eCAADe 2023 Digital Design Reconsidered, Volume 1: Proceedings of the 41st Conference on Education and Research in Computer Aided Architectural Design in Europe, Sep. 20-22, 2023, Graz University of Technology, Graz, Austria

[5] S. Ahlquist, J. Lienhard, J. Knippers, and A. Menges, "Exploring material reciprocities for textile-hybrid systems as spatial structures," in Prototyping Architecture: The Conference Papers, Feb. 2013, pp. 187-210.

[6] H. C. Koch, D. Schmelzeisen, and T. Gries, "4D textiles made by additive manufacturing on pre-stressed textiles—An overview," in Actuators, vol. 10, no. 2, p. 31, Feb. 2021.

[7] D. Jourdan, M. Skouras, E. Vouga, and A. Bousseau, "Printing-on-fabric meta-material for self-shaping architectural models," in Advances in Architectural Geometry 2020.

[8] L. Aldinger, G. Margariti, A. Körner, S. Suzuki, and J. Knippers, "Tailoring Self-Formation fabrication and simulation of membrane-actuated stiffness gradient composites," in Proceedings of IASS Annual Symposia, vol. 2018, no. 18, pp. 1-8, International Association for Shell and Spatial Structures (IASS), Jul. 2018.

[9] Y. Berdos, A. Agkathidis, and A. Brown, "Architectural hybrid material composites: computationally enabled techniques to control form generation," Architectural Science Review, vol. 63, no. 2, pp. 154-164, 2020.

[10] P. H. Bhagat and B. Gursoy, "Stretch-3D Print-Release: Formal descriptions of shape-change in 3D printed shapes on stretched fabric," in 40th Conference on Education and Research in Computer Aided Architectural Design in Europe, eCAADe 2022, pp. 301-310.

[11] T. Vivanco, A. Valencia, and P. F. Yuan, "4D printing: computational mechanical design of bi-dimensional 3D printed patterns over tensioned textiles for low-energy three-dimensional volumes," in Proceedings of the 25th CAADRIA Conference, 2020.

[12] D. B. Sitotaw, D. Ahrendt, Y. Kyosev, and A. K. Kabish, "Additive manufacturing and textiles—state-of-the-art," Applied Sciences, vol. 10, no. 15, p. 5033, 2020.

[13] M. Palma, „rs_gh“. Zenodo, Juli 01, 2024. doi: 10.5281/zenodo.12607863.